Taylor & Francis
Taylor & Francis Group

Journal of Toxicology and Environmental Health, Part A
Current Issues

ISSN: 1528-7394 (Print) 1087-2620 (Online) Journal homepage: https://www.tandfonline.com/loi/uteh20

# Exposure to graphene nanoparticles induces changes in measures of vascular/renal function in a load and form-dependent manner in mice

K. Krajnak, S. Waugh, Ab Stefaniak, D Schwegler-Berry, Ka Roach, M Barger & Jr. Roberts

**To cite this article:** K. Krajnak, S. Waugh, Ab Stefaniak, D Schwegler-Berry, Ka Roach, M Barger & Jr. Roberts (2019) Exposure to graphene nanoparticles induces changes in measures of vascular/renal function in a load and form-dependent manner in mice, Journal of Toxicology and Environmental Health, Part A, 82:12, 711-726, DOI: 10.1080/15287394.2019.1645772

**To link to this article:** https://doi.org/10.1080/15287394.2019.1645772

JOURNAL OF TOXICOLOGY AND ENVIRONMENTAL HEALTH, PART A
2019, VOL. 82, NO. 12, 711–726
https://doi.org/10.1080/15287394.2019.1645772

Taylor & Francis
Taylor & Francis Group



# Exposure to graphene nanoparticles induces changes in measures of vascular/renal function in a load and form-dependent manner in mice

K. Krajnak[a], S. Waugh[a], Ab Stefaniak[b], D Schwegler-Berry[a], Ka Roach[c], M Barger[a], and Jr. Roberts[a]

[a]Health Effects Laboratory Division, National Institute for Occupational Safety and Health, Morgantown, WV, USA; [b]Respiratory Health Division, West Virginia University, Morgantown, WV, USA; [c]Department of Physiology

**ABSTRACT**

Graphenes isolated from crystalline graphite are used in several industries. Employees working in the production of graphenes may be at risk of developing respiratory problems attributed to inhalation or contact with particulate matter (PM). However, graphene nanoparticles might also enter the circulation and accumulate in other organs. The aim of this study was to examine how different forms of graphene affect peripheral vascular functions, generation of reactive oxygen species (ROS) and changes in gene expression that may be indicative of cardiovascular and/or renal dysfunction. In the first investigation, different doses of graphene nanoplatelets were administered to mice via oropharyngeal aspiration. These effects were compared to those of dispersion medium (DM) and carbon black (CB). Gene expression alterations were observed in the heart for CB and graphene; however, only CB produced changes in peripheral vascular function. In the second study, oxidized forms of graphene were administered. Both oxidized forms increased the sensitivity of peripheral blood vessels to adrenoreceptor-mediated vasoconstriction and induced changes in ROS levels in the heart. Based upon the results of these investigations, exposure to graphene nanoparticles produced physiological and alterations in ROS and gene expression that may lead to cardiovascular dysfunction. Evidence indicates that the effects of these particles may be dependent upon dose and graphene form to which an individual may be exposed to.

**KEYWORDS**

Graphene inhalation; oxidative stress; gene expression; vascular dysfunction

## Introduction

Various forms of graphene generated from crystalline graphite are being widely used in the electronics industry (Sanchez et al. 2012). At least six different forms of graphene have been manufactured, described, and employed by the electronics and health industries. These forms include monolayer graphene, few-layer graphene (FLG), ultrathin graphite, graphene oxide, reduced graphene oxide and nano-graphene oxide (Sanchez et al. 2012). The utilization of graphene has expanded, attributed to its material properties which include superior strength, flexibility and ability to conduct electrical signals (Sanchez et al. 2012; Smith 2017). However, with increased usage and production of graphene nanoparticles and nano-sheets, there is a potential for a rise in exposure in the workplace. Workers involved in the manufacturing of electronics, batteries, printable inks, filters, automotive parts, medical devices, and supercapacitors may be exposed to graphene by inhalation (O'Mahony et al. 2019; Sanchez et al. 2012; Sang Tran, Dutta, and Roy Choudhury 2019). In addition, construction workers (concrete preparation) and scientists devising new methods for delivery of chemotherapeutic drugs may potentially be exposed to these particles via inhalation or dermal contact (Bussy et al. 2015; Dasari Shareena et al. 2018; Feng and Liu 2011; Sanchez et al. 2012; Su et al. 2016; Tabish, Zhang, and Winyard 2018; Zhang et al. 2016a). There are currently few workplace exposure assessment studies available for graphene materials. However, a human airway deposition modeling study demonstrated that graphene nanoparticles exhibit the propensity to deposit in the upper airways of workers (Su et al. 2016). Further, several animal experiments noted that graphene materials were in the respirable size range (Han et al. 2015; Kim et al. 2016; Ma-Hock et al. 2013; Shin et al. 2015; Su et al. 2016). In addition, *in vivo* studies also showed translocation of graphene materials to other organs such as spleen

**CONTACT** K. Krajnak ksk1@cdc.gov National Institute for Occupational Safety and Health, Morgantown, WV 2650, USA
Color versions of one or more of the figures in the article can be found online at www.tandfonline.com/uteh.

and liver following pulmonary exposure (Mao et al. 2016). It is worthwhile noting that several investigators reported that pulmonary nanoparticle exposures *in vivo* produce adverse effects on the cardiovascular system (Donaldson et al. 2013).

Graphene oxide (GO) GO is manufactured by chemically oxidizing crystalline graphite resulting in the chemical attachment of oxygen-containing functional groups onto every graphene sheet in the material. A process of thermal reduction is then applied to the material to generate the rGO material. This process restores electrical conductivity and may alter other properties of the molecule, including a reduction in density relative to the parent compound that occurs during the reduction process (Sanchez et al. 2012). Both of these oxidized forms of graphene were found to induce pulmonary inflammation (Bengtson et al. 2017; Duch et al. 2011; Li et al. 2013; Shurin et al. 2014). Acute inhalation of unoxidized graphene particles was also found to induce pulmonary inflammation (Ma-Hock et al. 2013; Roberts et al. 2016). However, inhalation of a number of other nanoparticles, and induction of pulmonary inflammation, is also associated with detrimental effects on a number of other systems in the body (Kermanizadeh et al. 2016). Investigators examining the influence of titanium dioxide inhalation at concentrations that do not induce a major pulmonary response, exerted actions on peripheral and cardiovascular functions (LeBlanc et al. 2010; Nurkiewicz et al. 2006). Therefore, determining if there are alterations in cardiovascular function in response to graphene inhalation may serve as a sensitive indicator of toxicity following nanoparticle exposure.

To assess the effects of different forms of graphene, an established model of pulmonary exposure to nanoparticles was used to test the hypothesis that changes in peripheral vascular function, and alterations in other factors involved in regulating blood pressure and cardiovascular function are affected by exposure to graphene nanoparticles (Porter et al. 2010; Roberts et al. 2016). Roberts et al. (2016) examined the effects of pulmonary exposure to these three different sized graphite nanoplatelets found that exposure to all three forms induced acute inflammation of the lungs, but inflammation persisted up to 1 month post-exposure in mice exposed to nanoplatelets with larger dimensions (Gr5 and 20) (Roberts et al. 2016). It was thus of interest to determine if changes in cardiovascular function occurred that were associated with different sized particles and different forms of graphene. The goal of this investigation was to specifically examine graphene sheets of three different sizes and compare the results obtained to those obtained with exposure to a dispersion medium (DM control), and those obtained with exposure to carbon black (CB) nanoparticles which were used as a carbon-based reference material, on peripheral cardiovascular responsiveness and relationship to changes in expression of factors that influence blood pressure (BP) and cardiovascular function. In addition, alterations in ROS levels in the heart and kidneys were determined as evidence of adverse effects attributed to nanoparticles (Ghio, Carraway, and Madden 2012).

## Methods

### Animals

Pathogen-free, male C57BL/6J mice, 8 weeks of age at arrival weighing approximately 23 g, were obtained from Jackson Laboratory (Bar Harbor, ME). Mice were allowed to acclimate to the facilities for 1 week prior to the beginning of the experiment. Mice were individually housed in polycarbonate ventilated cages with HEPA-filtered air, in humidity and temperature-controlled room, under a 12:12 hr light/dark cycle. All animals were provided with food (Harlan Teklad Rodent Diet 7913; Indianapolis, IN) and tap water *ad libitum*. All housing and exposure facilities were in compliance with the AAALAC International. All procedures were approved by Centers for Disease Control and Prevention/National Institute for Occupational Safety and Health (Morgantown) Animal Care and Use Committee and in compliance with ethical standards put forth by AAALAC International, the Animal Welfare Act and the Office of Laboratory Animal Welfare (OLAW). For all experiments, an n = 6 mice per group was used.

### Particle characterization and exposures

Three different sizes of non-oxidized graphite nanoplatelets and two oxidized forms of graphene were provided by Cabot Corp., Billerica, MA. Printex 90® (Degussa Heuls, Germany) carbon black (CB), was used as a reference material control. Samples of

graphene were manufactured to have approximate particle dimensions of 1, 5 or 20 μm lateral (referred to Gr1, 5, or 20, respectively) and thickness of 1–2, 7, and 7 nm, respectively. Graphene oxide (GO), an oxidized intermediate material, and the reduced form of graphene oxide (rGO) were derived from the particles with similar dimensions to the Gr5 material. CB, Gr1, Gr5, and Gr20 were characterized as previously reported (Roberts et al. 2016). GO and rGO were similarly characterized. Briefly, density was measured by the tap density method and primary particle size was reported by the manufacturer. The size was confirmed by field emission scanning electron microscopy (FESEM) and illustrated in Figure 1. The surface area of the dry powder form was measured by the Brunauer, Emmett, and Teller (BET) method (Materials AsoT 2002, ASTM B922-02).

Particles (40 μg) were suspended in 50 μl of a well-characterized dispersion media (DM; containing 0.6 mg/ml mouse serum albumin, 0.01 mg/ml dipalmitoyl phosphatidylcholine in phosphate-buffered saline) (Sager et al. 2007). The dosages were selected based upon a number of previous studies examining the influence of carbonaceous nanomaterials following oropharyngeal aspiration (Porter et al. 2010; Roberts et al. 2016). Samples were sonicated for 15 sec at 10 W using a probe sonicator and utilized

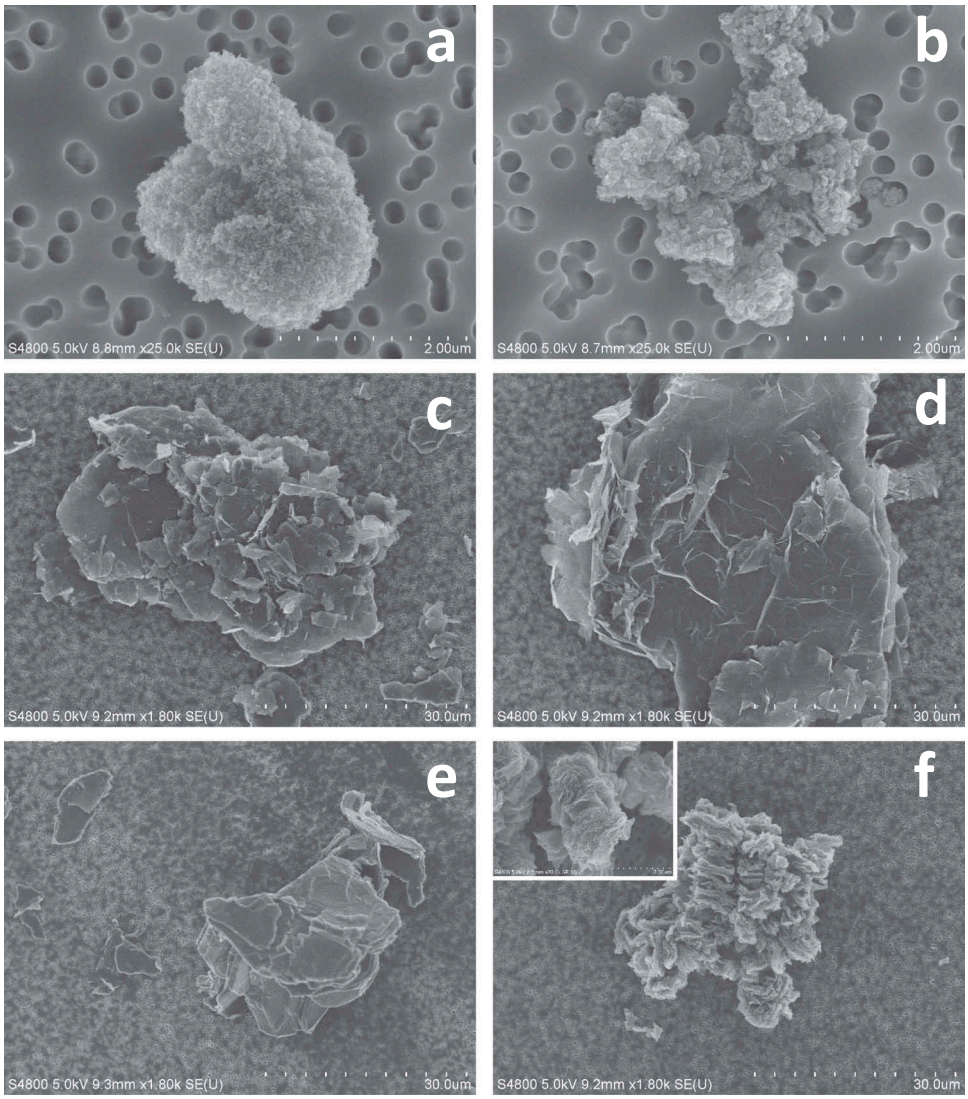


**Figure 1.** Field emission scanning electron micrographs of agglomerates of particles prepared in dispersion medium (DM) for oropharyngeal aspiration studies: CB (a) and Gr1 (b) are shown at a higher magnification (micron bar = 1 μm total, hatch marks = 0.1 μm apart) than Gr5 (c), Gr20 (d), GO (e), and rGO (f) (micron bar = 30 μm, hatches = 3 μm apart). A higher magnification of rGO is included (inset, F) demonstrating the layering of the rGO material.

immediately after preparation each day. The suspensions were characterized for agglomerate size in DM using microscopy to perform point counts on the particle and zeta potential of particles was measured using a zetasizer.

### Exposure

All mice were weighed prior to treatment by oropharyngeal aspiration. For Experiment 1, mice were anesthetized with 3% isoflurane and suspended by their incisors on a slanted board. Each animal's mouth was opened and tongue moved aside. A single 50 µl aliquot of dispersion media, or media containing 40 µg of the non-oxidized particles (Gr 1, 5 or 20 µm graphite nanoplatelets) or CB was pipetted onto the base of the tongue, and the animal remained in this position until two full breathes were taken no longer than 15 sec (Roberts et al. 2016). In study 2, animals were treated in an identical manner with DM, or oxidized forms of graphene GO or rGO. An n = 8 mice/condition was employed in both studies. Mice were allowed to recover from anesthesia before being placed back into their home cage in the colony room for 24 hr.

### Tissue collection

The day following exposure approximately 24 hr later each animal was weighed, anesthetized with a fatal dose of pentobarbital (100 mg/kg, i.p.) and euthanized by exsanguination. The ventral tail artery was dissected and stored in cold DMEM until use for microvessel studies. The kidneys and hearts were also extracted. The left ventricle heart was cut into two sections. One was used to measure RNA while the other portion utilized for determination of ROS levels. Similar to heart tissue, each kidney was placed in a separate tube and used for the same parameters to be measured. All tissues were frozen on dry ice and stored at-80°C until used for assays. The dose of graphene and time point (24 hr after exposure) were selected because previously Roberts et al. (2016) demonstrated that changes in RNA and other markers of inflammation in the lung were increased at 4 and 24 hr after a similar exposure. Because pulmonary inflammation persists at 24 hr after exposure at a dose of 40 µg (Roberts et al. 2016), and previous investigators demonstrated both physiological effects and gene expression alterations in the cardiovascular system are apparent 24 hr following exposure (Krajnak et al. 2011; LeBlanc et al. 2010; Nurkiewicz et al. 2006; Roberts et al. 2013), this time point was thus selected to assess the influence of graphene on the cardiovascular system.

### Measurements of vascular reactivity

To assess the effects of pulmonary graphene exposure on peripheral vascular function, the ventral tail artery was dissected, mounted on pipettes and placed in a microvessel chamber (Living Systems Instrumentation, Catamount Research and Development, Inc.). Artery segments were pressurized and maintained at 60 mm Hg. Phenylephrine (PE: Cat 207240200) and acetylcholine (Ach: Cat A6625) were purchased from Sigma Aldrich (Indianapolis, IN). Vasoconstriction in response to the α-1-assessing adrenoreceptor agonist, PE, was monitored after applying the drug in half-log increments (−10 to −6.5 M) and the internal diameter was recorded after the vessel equilibrated (approximately 5 min). If the artery reached a 50% constriction from the basal diameter, no additional PE was added. Data were calculated as % change from baseline. After assessing the effects of PE, arteries were rinsed until they returned to their original baseline. Arteries were then re-constricted to 50% of baseline with PE and acetylcholine (ACh) was applied to the bath to induce a re-dilation. Ventral tail arteries do not have endogenous basal tone, such that these were pre-constricted to assess sensitivity to ACh-induced re-dilation. As with PE, ACh was added in progressively increasing doses (half-log increments from −9 to −5.5) and alterations in internal diameter recorded.

### Quantitative reverse-transcriptase polymerase chain reaction-PCR (qRT-PCR)

The procedures for RNA isolation, amplification and transcription were described previously (Krajnak et al. 2011). Briefly, tissues were homogenized and RNA was isolated by centrifugation using the Rneasy Lipid Tissue kit (Cat # 74804; Qiagen, Germantown, MD). One µg RNA was used for reverse transcription using the High Capacity cDNA reverse-Transcriptase kit (Cat 42–688-13; Life Technologies Corp, Waltham,

MA), and amplification performed using probes from Universal Roche Probe Library (Cat # 04683650001; Roche Diagnostics, Indianapolis, IN). All PCR was performed using FS Universal SYBR Green master ROX 5 and Faststart Universal Probe Master Mix (Cat 4913850001 and 4913957001, respectively; Sigma-Aldrich, St Louis, MO). Ribosomal 18 s (18s) was used as a control to determine if there were equivalent levels of RNA in each sample. Other transcripts that were measured are presented in Table 1. PCR was performed in an Applied Biosystems 7500 thermocycler and a Step-One-Plus analyzer (Applied Biosystems, Foster City, CA) and the critical threshold (CT) of amplification for each transcript was used as a measure of transcript levels. A standard curve for each gene was also run (by increasing the concentration 10-fold for each standard) to determine the efficiency of each PCR assay. The exposure-induced change in CT (ΔCT) was calculated by subtracting the mean CT of the DM group from each sample. The fold change was calculated using the following formula (efficiency of the PCR run$^{\Delta CT}$). The fold change was used for statistical analyses.

### Tissue $N_{ox}$ and $H_2O_2$ concentrations

Heart and kidney tissues were homogenized in 1 ml of 0.1 M phosphate-buffered saline (PBS; pH 7.2) containing protease inhibitor, centrifuged (Nox: 15 min at 4500 g; H2O2: 100,000 x g for 30 min, both at 4°C) and the supernatants were removed and assayed for nitrate/nitrite ($N_{ox}$) and hydrogen peroxide ($H_2O_2$) was measured using the nitrate/nitrite kit (Cat # 780001; Caymen Biologics, Ann Arbor, MI). In Experiment 2, Fluoro $H_2O_2$ kit (Cat FLOH100; Cell Technologies, Inc, Fremont CA) was utilized to measure $H_20_2$ as the lab no longer had access to an ultracentrifuge and homogenized samples were all centrifuged at 4500 g. Assays were performed using the manufacturer's protocols. To account for potential differences in the size of the tissue that $N_{ox}$ and $H_2O_2$ were isolated from, the tissue pellet remaining after homogenization and centrifugation was resuspended in 1 ml of PBS and 10 ul was assayed using a bicinchoninic acid (BCA) protein assay (Pierce Chemicals, Dallas TX). Concentrations of ROS expressed as concentration/μg protein.

**Table 1.** Transcripts quantified by qRT-PCR in the heart and kidney. All transcripts were measured using probes from the Roche library.

| Heart | Kidney |
|---|---|
| Angiotensin converting enzyme (ACE) | Dopamine receptor 1a (Drd1a) |
| Hypoxia induced factor-1a (HIF1a) | Dopamine receptor 2 (Drd2) |
| Metallothionin-1 (Mt1) | Chemokine (C-X-C motif) ligand 14 (Cxcl14) |
| BAD (pro-apoptotic) | Dopamine receptor 5 (Drd5) |
| BAX (pro-apoptotic) | Cyclic-AMP response-element binding protein (CREB) |
| $BCl_2$ (repression of apoptosis) | Tissue inhibitor of metalloproteinase-1 (TIMP1) |
| Fibronectin-1 (FN1) | Endothelial nitric oxide synthase ($NOS_2$) |
| Collagenase-1 (Col1a1) | Inducible nitric oxide synthase ($NOS_3$) |

### Statistical analyses

All statistical analyses were performed with Jmp 13.2.0 (2016; SAS Institute, Cary NC, 2016). Microvessel data (mean internal diameter) were analyzed using a 5 (treatment) x 5 (dose) repeated measures (RM)-ANOVA for experiment 1 and a 3 (treatments) x 9 (dose) RM-ANOVA for Experiment 2. Appropriate post-hoc comparisons were conducted using one-way ANOVAs or Student's t-tests, to assess pairwise comparisons. The effective dose that generated a 50% change in vascular diameter ($ED_{50}$) was calculated by fitting the dose-response from each mouse, using a non-linear fit function (Prism 5.0 for Windows, 2001–2007; Prism Inc, San Diego, CA), which also determined the $ED_{50}$. The $ED_{50}$ for each group was then analyzed using a one-way ANOVA (Experiment 1) or a Student's t-test (Experiment 2). Other data were analyzed using one-way ANOVAs followed by t-test tests to determine if measures were different from DM controls. All data are reported as the mean ± SEM, and differences with a $p < .05$ considered significant. Graphs were made using Prism 5.0 for Windows.

## Results

### Particle characterization

Particle morphology is illustrated in Figure 1. CB is spherical in shape while, Gr1, 5, and 20 are in platelet forms, and vary in primary particle size.

GO displays similar structural morphology to Gr5, while rGO has a more separated layered and accordion-like structure. Characterization of both the dry powder form of particles and suspension is reported in Table 2. Gr1 and rGO had the greatest surface area followed by CB. Gr5 and GR20 were similar in terms of surface area. The surface area was not measured for GO due to concern for exothermic decomposition during degassing in the BET method; however, similarities in size, morphology, and density suggest that it would be similar to the Gr5 sample, a similar particle from which the GO was derived. The density of rGO was approximately an order of magnitude lower than Gr20, which in turn was approximately an order of magnitude lower than Gr1, 5, and CB which were similar to each other. Sonication was found to disrupt the primary particle size of the largest sample, Gr20, to a degree, and it also represented the material with the widest particle size range. It is important to note that because of its low density, dosing on an equal mass basis and taking into consideration particle size, 40 µg of the rGO results in a significantly greater particle load by number delivered to the lungs when compared to the other graphene-based materials.

### Experiment 1. Gr1, 5 and 20

*Microvessel*: Vascular responses to the varying concentrations of Gr are presented in Figures 2a–d. Oropharyngeal aspiration of different sized graphene nanoplates did not markedly affect the sensitivity of the ventral tail artery to α1-adrenoreceptor-induced vasoconstriction (Figure2a). However, exposure to CB significantly increased sensitivity to PE-induced constriction as compared to DM controls, particularly at the highest PE-log dose (Figure2b). Although the $ED_{50's}$ appeared to be lower in CB-treated animals compared to mice treated with Gr1 and 5, these differences were not significant. Re-dilation in response to ACh was highly variable and analyses of concentration-dependent re-dilation were not significantly different between groups (Figure 2c–d).

*$N_{ox}$ and $H_2O_2$ concentrations*: Nitrate/nitrite ($N_{ox}$) levels in heart and kidney were not significantly affected by any of the exposures (Table 3). Hydrogen peroxide ($H_2O_2$) concentrations also were not significantly different between DM and non-oxidized graphite nanoplatelet-treated animals in the heart Table 3). However, $H_2O_2$ concentrations were significantly higher in CB compared to DM-administered mouse kidneys. In addition, $H_2O_2$ levels were lower in kidneys of Gr20 than CB-exposed and DM animals; however, only the difference between the CB and Gr20 exposed mice was significantly different.

*qRT-PCR*: Treatment-induced changes in transcript levels in relation to DM are presented in Figure 3. In the heart (Figure 3a), exposure to all particles significantly increased type 1a1 collagenase (Col1a1) expression. Exposure to Gr5 also significantly elevated chemokine Cxcl14 in the heart. In the kidney (Figure 3b), exposure to CB resulted in a significant rise in chemokine ligand 24 (Ccl24). Gr exposure, regardless of size, did not

**Table 2.** Particle characteristics.

| Particle | Primary Particle Size | Density (g/ml) | Specific Surface Area ($m^2/g$) ± SEM | Mean Agglomerate Size in DM Following Sonication (µm) ± SEM | Zeta Potential in DM (mV) ± SEM |
|---|---|---|---|---|---|
| CB | 15–20 nm | 0.180 | 334.0 ± 2.9 | 1.16 ± 1.18 | −12.6 ± 0.6 |
| Gr1 | 1–2 µm lateral,1–2 nm thickness | 0.200 | 747.1 ± 4.4 | 1.60 ± 1.58 | −15.1 ± 0.8 |
| Gr5 | 5 µm lateral,7 nm thickness | 0.190 | 106.5 ± 1.1 | 4.30 ± 4.32 | −14.9 ± 0.8 |
| Gr20 | 20 µm lateral,7 nm thickness | 0.070 | 115.5 ± 8.4 | 7.28 ± 13.4 | −17.1 ± 1.2 |
| GO | 5 µm lateral,7 nm thickness | 0.420 | N.D. | 4.89 ± 6.55 | −14.1 ± 1.1 |
| rGO | Not Reported | 0.003 | 650 | 4.07 ± 3.89 | −12.5 ± 0.7 |

Density and primary particle size were measured by the tap density method. The specific surface area was measured by BET method for all particles with the exception of GO (N.D., not determined) as per recommendation due to potential reactivity in the assay (1–3 measures per sample ± standard error). Mean agglomeration in DM was determined morphometrically using point count methods microscopically for the Gr5, Gr20, GO, and rGO samples, and both microscopically and with validation by dynamic light scattering for the smallest particles CB and Gr1 particles. Point counts are the mean of ~200–500 counts per sample ± standard deviation. Agglomerates ranged in size up to 2, 2, 60, 300, 40, and 70 µm for CD, Gr1, gr5, gr20, GO, and rGO, respectively. Zeta is reported as the average of two separate measures per sample.

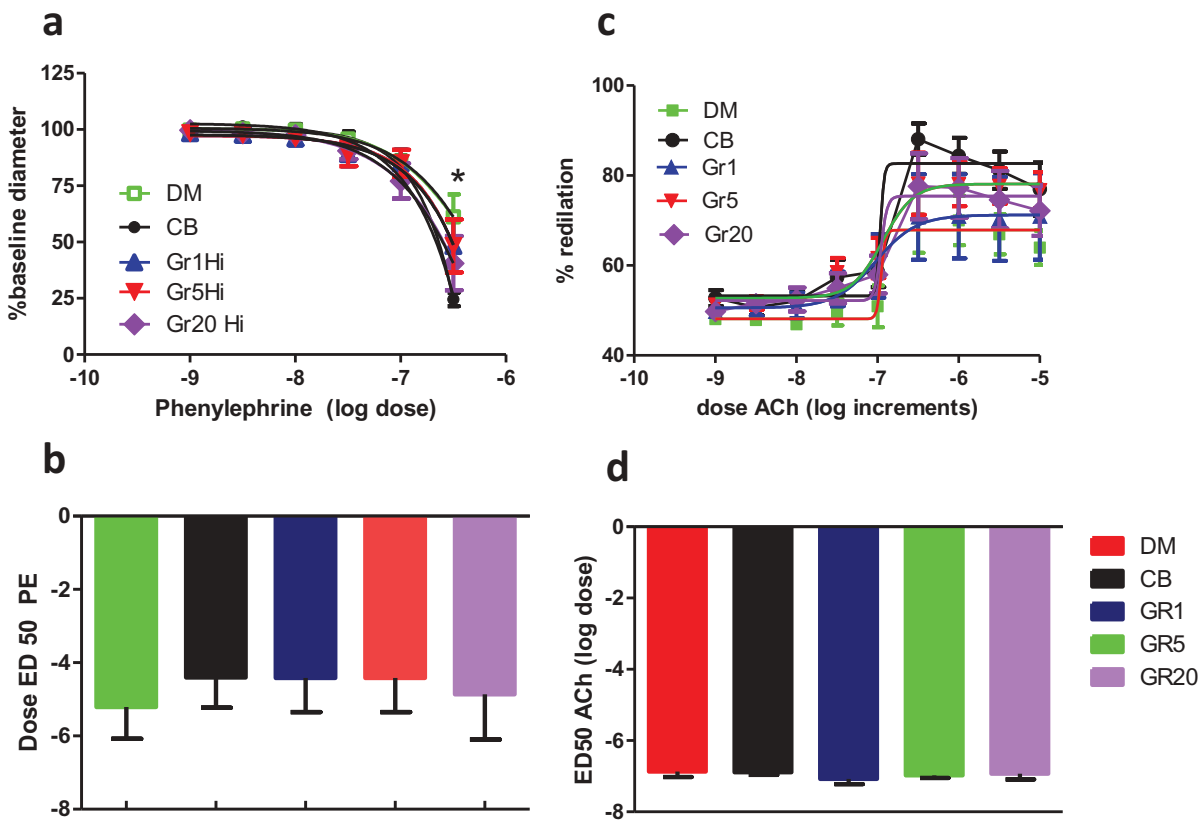


**Figure 2.** These graphs show vascular responses to the α1-adrenoreceptor agonist PE (a and b) and ACh (c and d). Exposure to Gr1, 5 and 20, did exert significant effects on PE-induced vasoconstriction (a). However, mice exposed to CB showed a greater vasoconstriction than those exposed to DM in response to PE at the highest dose (*$p < .05$). Although the $ED_{50}$ to PE appeared to be lower in CB, Gr1, and Gr5-treated mice, these differences were not significant (b). Figure 1a and D illustrate vasodilation in response to ACh. There were no marked changes in dose-dependent dilation (c) in response to ACh or in the $ED_{50}$ (d).

**Table 3.** Concentrations of $N_{ox}$ and $H_2O_2$ in the heart and kidney after exposure to different dosages of graphene (Experiment 1: clear boxes) or oxidized graphene (Experiment 2: shaded boxes).

| | $N_{ox}$ (nM/µg protein) | | H202 (nM/µg protein) |
|---|---|---|---|
| condition | Heart | Kidney | Heart |
| DM | 0.20 | 0.013 | 0.44 |
| | (0.02) | (0.005) | (0.1) |
| CB | 0.22 | 0.012 | 0.50 |
| | (0.02) | (0.001) | (0.02) |
| Gr1 | 0.20 | 0.011 | 0.56 |
| | (0.02) | (0.001) | (0.15) |
| Gr5 | 0.18 | 0.010 | 0.40 |
| | (0.01) | (0.002) | (0.10) |
| Gr20 | 0.21 | 0.010 | 0.50 |
| | (0.03) | (0.003) | (0.20) |
| DM-GO | 0.51 | 2.24 | 0.48 |
| | (0.16) | (0.68) | (0.11) |
| GO | 0.55 | 5.05 | 0.24 |
| | (0.17) | (1.89) | (0.11) |
| DM-rGO | 0.56 | 4.68 | 0.30 |
| | (0.17) | (1.36) | (0.12) |
| rGO | 0.69 | 2.36 | **0.94** |
| | (0.20) | (1.12) | **(0.28)*** |

Data are presented as the mean (SEM). Values significantly different than those measured in DM-treated animals are designated in bold type (*$p < 0.05$)

exert a significant effect on any of the transcripts measured in the kidney.

### *Experiment 2. GO vs rGo*

*Microvessel*: Figure 4 shows vascular responses to PE and ACh after exposure to GO. There were no marked exposure-related differences in response to PE when the concentration-dependent vasoconstriction was analyzed by repeated-measures ANOVAs (Figure 4a). Analysis of the $ED_{50}$ in response to PE demonstrated that there was a significant difference between DM and GO-treated mice with arteries from GO-treated animals being more sensitive to PE-induced constriction than arteries from DM controls (Figure 4b; mean ± sem; DM: $10^{-6.92 \pm 0.35}$; GO $10^{-7.14 \pm 0.12}$ mM PE). ACh-induced re-dilation is presented in Figures 4c, d. GO exposure did not markedly alter the concentration–response relationship or $ED_{50}$ ACh.

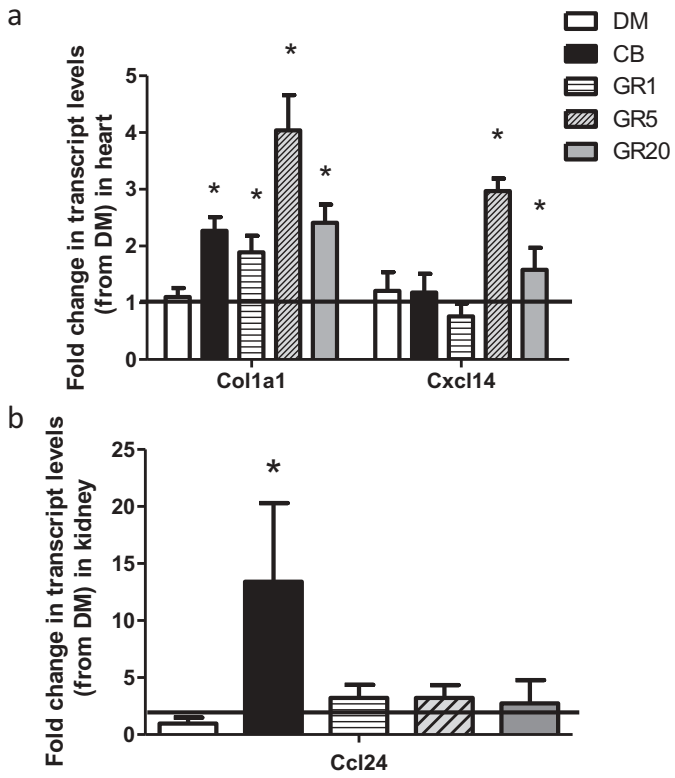


**Figure 3.** Transcripts that showed significant changes in response to Gr or CB exposure. In the heart (a), exposure to all particles enhanced the expression of *Col1a1*. Exposure to Gr5 and Gr20 increased expression of *Cxcl14*. In the kidney, *Ccl24* was elevated in CB-exposed mice. All significant differences (*p < .05) are as compared to DM controls.

Vascular responses to PE and ACh after rGO are presented in Figure 5. Arteries from mice exposed to rGO were more sensitive to PE-induced vasoconstriction than those exposed to air (Figures 5a,b). Although arteries from rGO-treated mice appear to be less sensitive to ACh-induced re-dilation, these differences were not significant (Figures 5c,d).

*$N_{ox}$ and $H_2O_2$ concentrations*: Neither exposure to GO nor rGO exerted a marked effect on $N_{ox}$ concentrations in heart or kidney (Table 3). $H_2O_2$ concentrations in the heart were not significantly different in DM and GO-exposed mice. However, $H_2O_2$ was markedly higher in heart tissue of animals exposed to rGO as compared to those exposed to rDM-GO. Kidney $H_2O_2$ concentrations were at the lower level of detectability of the assay in samples collected from all groups and therefore not reported.

*qRT-PCR*: Figures 6a,b illustrate transcript levels in the heart after exposure to GO or rGO. *FN1* was significantly decreased and *Mt1a* was elevated in mice exposed to GO as compared to DM (Figure 6a) *Ace* also was significantly increased in GO-exposed mice. Mice exposed to rGO displayed a rise in *Ace, Bcl2, and Mt1*, and a reduction in *Fn1* and *Nos2* (Figure 6b). Figure 7 shows changes in transcript levels in the kidney after exposure to GO or rGO. Cxcl14 and CREB were increased in the kidney of GO compared to DM-exposed mice (Figure 7a). Figure 7b demonstrates changes in transcript levels in kidneys after exposure to rGO. *Drd1* and *CREB* were significantly elevated and *Drd2, FN1*, and *Col1a1* were reduced as compared to DM controls.

## Discussion

The global market for graphene and products that incorporate is growing rapidly. Graphene is being used in a number of different industries to improve the product longevity and conductivity including but not limited to electronics, sensors, energy storage, and composites (Sanchez et al. 2012; Smith 2017). The goal of this study was to examine graphene nanoparticles of different sizes

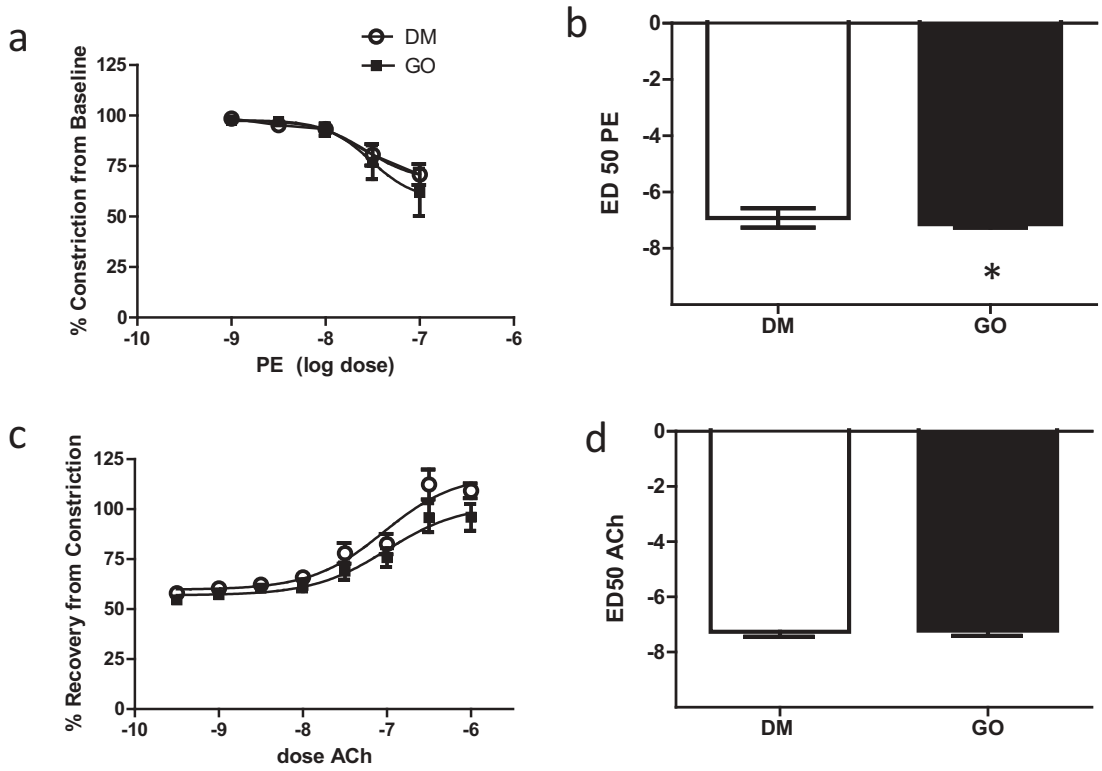


**Figure 4.** Dose-dependent vasoconstriction in response to PE (a and b) and re-dilation in response to ACh (c and d) in GO-treated mice. Exposure to PE resulted in a significant reduction in $ED_{50}$ in GO-treated mice (b; the concentration of PE needed to induce a 50% constriction was diminished; *p < .05). There were no significant differences in ACh-induced re-dilation (c and d).

and different forms to determine if pulmonary exposure resulted in changes in peripheral vascular function and markers of acute tissue responses in heart and kidney of rats. This study examined the effects of installation of graphene nano-platelets on specific markers that previously have been associated with the development of changes in cardiovascular function with prolonged exposures (Krajnak et al. 2011; Roberts et al. 2014, 2013, 2016). Data demonstrated that an acute exposure to non-oxidized forms of graphene did not significantly alter the peripheral vascular function or oxidative stress parameters, but affected transcription of a few genes involved in inflammation and remodeling in the heart and kidney. It is worthwhile noting that incubation of mouse lymphoma cells with graphene failed to significantly affect LDH activity, ROS levels and gene expression of catalase and superoxide dismutase, indicating that although graphene may be genotoxic, cytotoxic or mutagenic, it does not induce oxidant stress in this cell type *in vitro* (Demir and Marcos 2018). Although oxidative stress was not altered by pulmonary instillation of graphene nanosheets in the current study, GO exposure produced alterations in the expression of specific factors associated with inflammation (e.g., *MT1a, CCL24, Cxcl14*), cell signaling (*Creb*) and remodeling factors (*Col1a1, Fn1*) in the heart and kidney. In contrast, exposure to rGO resulted in increased-sensitivity to PE-induced vasoconstriction (i.e., less PE was needed to induce a vasoconstriction) which might potentially contribute to a short-term change in blood pressure (Krajnak et al. 2011). rGO exposure also resulted in a rise in $H_2O_2$ concentrations in the heart, and changes in gene transcription similar to those seen with exposure to GO. In the kidney, rGO induced changes in the expression of transcripts involved in cell signaling (*Creb, Nos2, Drd1*, and *2*) and tissue remodeling (*Col1a1, Fn1*). Therefore, based upon the results of these studies, the oxidized forms of graphene exerted a more pronounced acute effect on vascular and renal systems than non-oxidized forms. Based upon our observations, future studies examining the influence of repeated exposures to

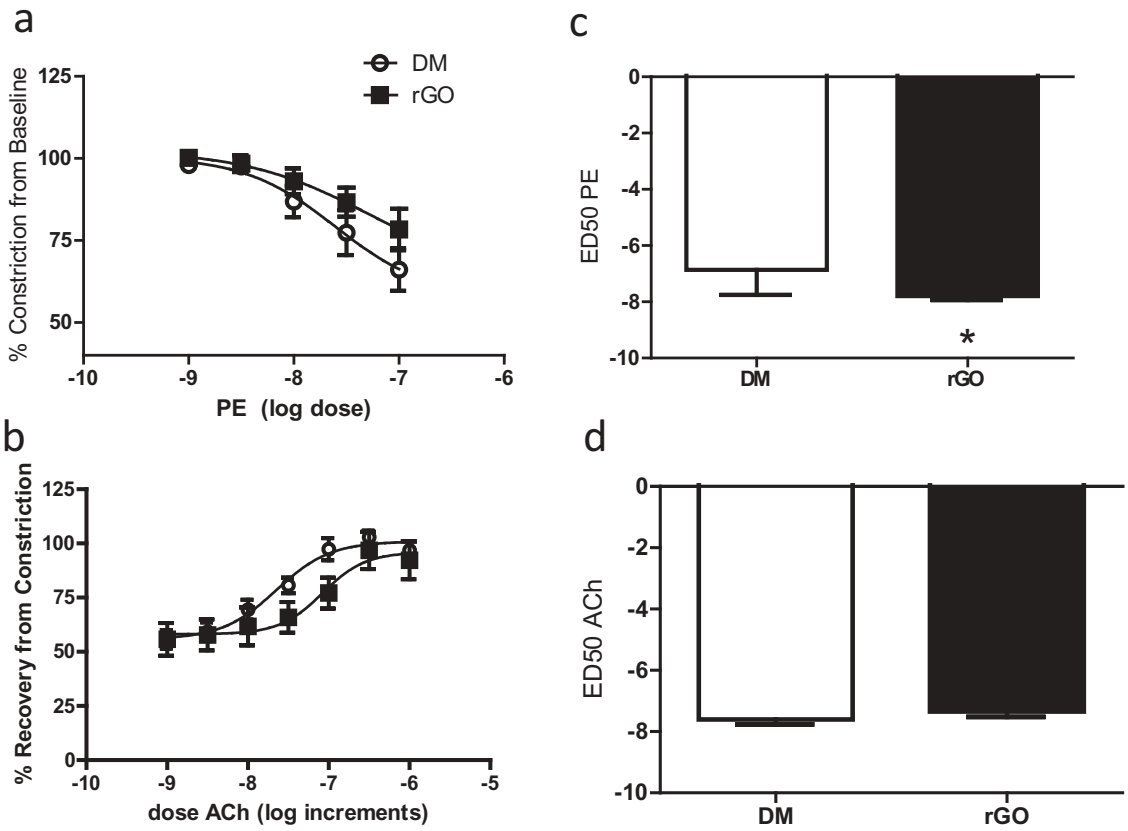


**Figure 5.** Dose-dependent vasoconstriction in response to PE (a and b) and re-dilation in response to ACh (c and d) in rGO-treated mice. Exposure to PE resulted in a significantly decreased $ED_{50}$ in rGO-treated mice (b; the concentration of PE needed to induce a 50% constriction was reduced; *p < .05). There were no marked differences in ACh-induced re-dilation (c and d).

oxidized graphenes and longer recovery times are warranted to determine if alterations seen in the current experiment were an acute response, or an indicative of disease development.

Cardiovascular function alterations that occur as a result of inhalation of toxicants are often associated with pulmonary inflammation (Krajnak et al. 2011; Nurkiewicz et al. 2006; Roberts et al. 2013). However, there are studies demonstrating that the cardiovascular system may be more sensitive and display a response to inhalation of toxins when there is little or no pulmonary response (LeBlanc et al. 2010; Nurkiewicz et al. 2006). Although pulmonary inflammation was not measured in these experiments, Roberts et al. (2016), assessing the effects of exposure to the same graphene nanoplatelets (i.e., Gr1, 5 and 20), found that exposure to these particles, or CB, resulted in a rise in neutrophils and LDH concentrations in bronchiolar lavage fluid. There were also increases in transcript levels for a number of pro-inflammatory factors in the lung after an acute exposure to Gr5 and Gr20 (Roberts et al. 2016). In addition, other investigators noted that oxidized forms of graphne may produce a greater acute pulmonary inflammation than the un-oxidized forms (Duch et al. 2011; Li et al. 2018; Shurin et al. 2014). Bengtson et al. (2017) reported the effects of a single exposure to similar particles from a different manufacturer and noted pulmonary inflammation was induced by the exposure that was maintained for up to 90 days. As mentioned previously, exposure to toxins or particles that induce pulmonary inflammation also often results in changes in cardiovascular function and systemic inflammation (Krajnak et al. 2011; LeBlanc et al. 2010; McKinney et al. 2012; Nurkiewicz et al. 2006; Roberts et al. 2014, 2013). Thus, the cardiovascular and renal effects observed in these experiments might be attributed to pulmonary inflammation induced by exposures to graphene.

In Experiment 1, where mice were treated with CB or one of the forms of Gr, the greatest effects

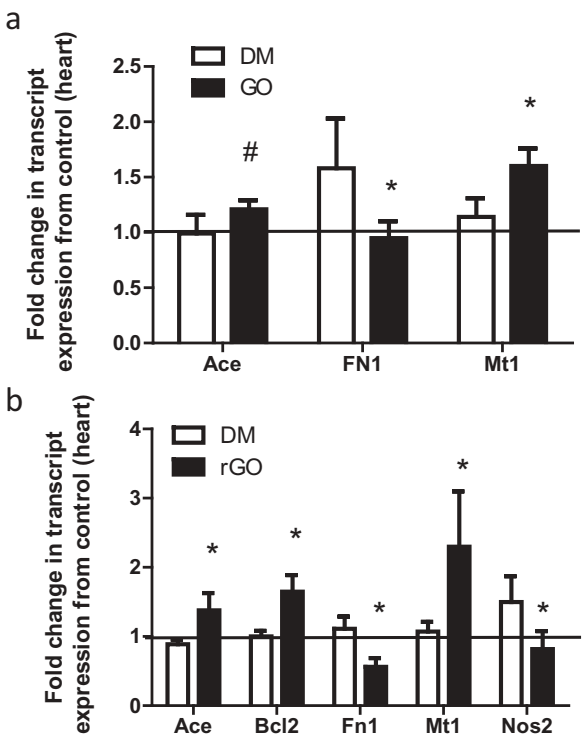


**Figure 6.** Transcript changes in heart tissue in response to GO (a) or rGO (b) exposure. Exposure to GO resulted in a rise in expression of *Ace* (# $p = .05$), and *Mt1a* (*p < .05). *Fn1* was reduced in mice exposed to GO (*p < .05). Exposure to rGO resulted in increases in expression of *Ace, Bcl*$_2$, and *Mt1*, and decreases in expression of *Fn1* and *Nos2* (* $p < .05$). All differences are as compared to DM controls.

were seen in animals treated with CB. Previous studies demonstrated that CB exposure induced an acute pulmonary inflammation (Lovinsky-Desir et al. 2016; Ma-Hock et al. 2013). However, results displaying the effects on the cardiovascular system are mixed, with some studies noting CB-induced alterations in the cardiovascular system while other investigators failed to detect effects (Holz et al. 2018; Saber et al. 2013). The different responses may be due to the fact that some studies generate black carbon particles by burning a carbon-producing source (Holz et al. 2018), while other studies, including this study use manufactured carbon black ultrafine particles (Croft et al. 2017; Roberts et al. 2016). The results of these studies are consistent with those showing that when compared to animals treated with DM, exposure to may induce factors that lead to pulmonary and/or cardiovascular dysfunction or disease (Nurkiewicz et al. 2006; Saber et al. 2013).

CB exposure resulted in an enhanced sensitivity to PE-induced vasoconstriction in ventral tail arteries. The changes may be attributed to increased load that occurs with exposure to nanoparticles of a smaller size (Roberts et al. 2013, 2016; Schinwald et al. 2012). Enhanced pulmonary inflammation and induction of inflammatory pathways such as ROS generation and increases the expression of pro-inflammatory cytokines (LeBlanc et al. 2010; Nurkiewicz et al. 2006), along with activation of the autonomic nervous system (Kan et al. 2014; Knuckles et al. 2012), might initiate systemic effects and alter responses of the cardio- and peripheral vascular systems to endogenous mediators of vascular function. The CB-induced alterations in vascular sensitivity to vasoconstricting and vasodilating factors also may contribute to the development of cardiovascular diseases. Studies examining the influence of CB-exposure on other vascular beds, including the microvasculature of the heart, demonstrated that exposure to CB induced elevation in oxidative activity and alterations in responsiveness to endothelial-mediated vasodilation (LeBlanc et al. 2010; Nurkiewicz et al. 2006).

Exposure to Gr did not significantly alter peripheral vascular responses to PE-induced vasoconstriction or ACh-mediated vasodilation. However, there was an elevation in a number of pro-inflammatory factors in the heart, which tended to be most prominent with exposure to Gr5 with some smaller changes following exposure to Gr20. In the kidney, exposure to non-oxidized graphenes did not markedly alter the expression of inflammatory factors. In the heart, exposure to all particles resulted in a rise in *Col1a1*, and Gr5- and Gr20-treated mice displayed changes in pro-inflammatory factor *Cxcl14*. These factors may be involved in repair and remodeling in tissues acutely (Lyu et al. 2015). However, a prolonged increase in the expression of these factors may be indicative of dysfunction (Erdely et al. 2013; Porter et al. 2010; Roberts et al. 2016). In Experiment 2, the effects of exposure to GO and rGO were examined. Although the administration of both particles resulted in a significantly lower $ED_{50}$ for PE, the change in the $ED_{50}$ with GO was small and may not have exerted significant effects on vascular physiology. However, the difference between $ED_{50}$ of DM and rGO-exposed mice was greater, with the $ED_{50}$ being significantly lower in the

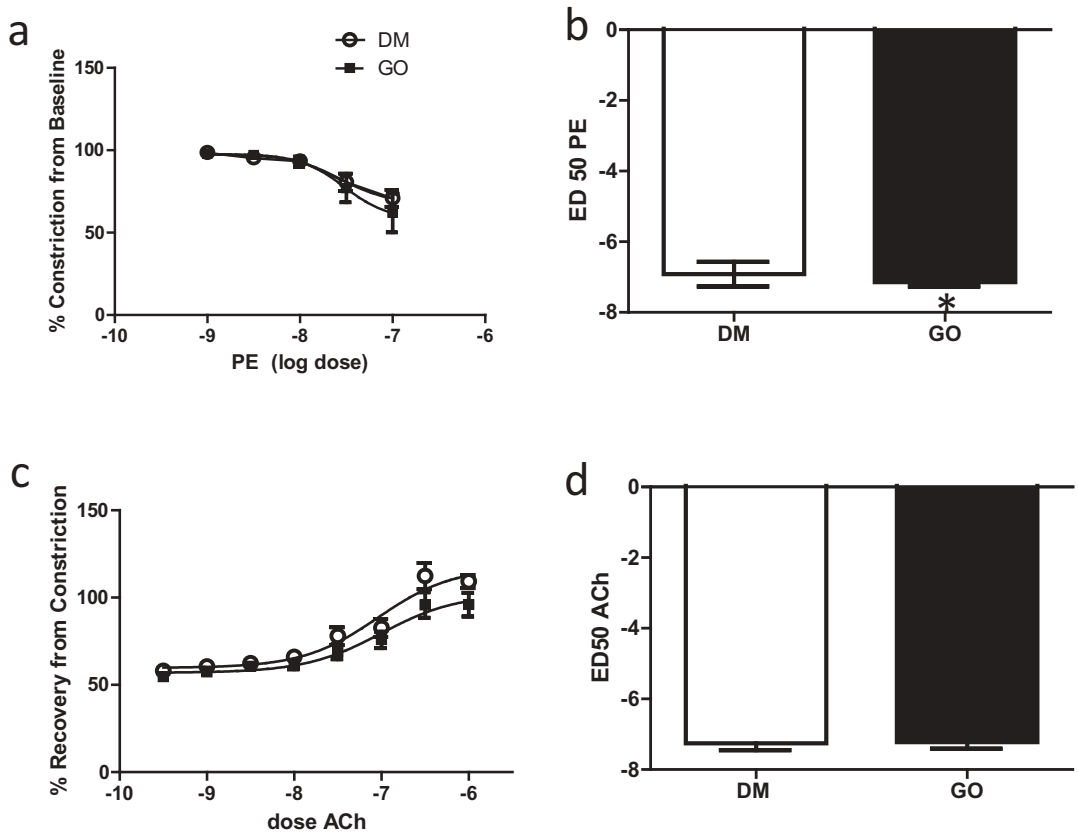


**Figure 7.** Changes in transcript levels in response to GO (a) and rGO (b) exposure in the kidney. Exposure to GO resulted in an elevation in *Cxcl14* (*p < .05) and *Creb* (#p = .05) expression, and reduction in *Col1a1* and *Ccl2* (*p < .05) transcript levels in the kidneys. In rGO-exposed mice, *Drd1* and *Creb* were increased and *Drd2, Fn1*, and *Col1a1* were reduced (*p < .05). All differences are as compared to DM controls.

exposed animals indicating that the tail artery was less sensitive to the influence of α1-noradrenergic-mediated vasoconstriction. Previously investigators observed that pulmonary exposure to nanoparticles induced an increased sensitivity to PE-induced vasoconstriction or reduced sensitivity to ACh-induced vasodilation after inhalation of other toxicants (Krajnak et al. 2011; McKinney et al. 2012; Roberts et al. 2014, 2013). Thus, it was surprising that treatment with rGO increased the sensitivity of the ventral tail artery to PE. Although $N_{ox}$ and $H_20_2$ concentrations were not evaluated in the peripheral vascular system, these measures were collected in heart tissue. There were no marked changes in $N_{ox}$ concentrations in the hearts of mice exposed to GO or rGO. However, there was a rise in $H_2O_2$ concentrations in heart tissue from rGO-exposed rats. Elevations in ROS, including, but not limited to $N_{ox}$ and $H_20_2$, are known to lead to damage of peripheral and cardiovascular tissues if maintained over time, and it is common to see changes in ROS levels in response to particle or toxin inhalation (Han et al. 2015; LeBlanc et al. 2010; Nurkiewicz et al. 2006). In fact, a number of studies demonstrated that particle-induced changes in vascular function, particularly reductions in endothelial-mediated vasodilation, are partially due to changes in ROS concentrations (Knuckles et al. 2012; LeBlanc et al. 2010; Nurkiewicz et al. 2006). Changes in $H_2O_2$, superoxide, peroxynitrite, and other ROS were found to interfere with nitric oxide (NO)-induced vasodilation. These other ROS alter NO activity by scavenging additional oxygen or NO by inhibiting nitric oxide synthase activity, and/or by reducing the bioavailability of tetrahydrobiopterin ($BH_4$). Both NO and $BH_4$ are needed to synthesize NO (Kotsonis et al. 1999; Xia et al. 1996).

Evidence suggests that increases in ROS levels in the physical presence of graphene nanoparticles may actually exhibit angiogenic properties (Mukherjee et al. 2015). Particle accumulation in

various tissues was not measured in these studies. However, there is evidence that there might be an accumulation of particles in various tissues after inhalation or intra-tracheal installation, and it has been postulated that these particles are being transported to other organs via the circulatory system (Liang et al. 2016; Kim et al. 2016; Lee et al. 2016). Cardiac transcript level alterations in Experiment 2 also suggest that exposure to GO and rGO induced the transcription of factors involved in the acute response of heart tissue to inhaled toxins. Both GO and rGO exposures stimulated increases in *Ace* and *Mt1a* expression in cardiac tissues. In addition, exposure to rGO induced a rise in *Bcl2* and reductions in *Fn1* and *Nos2* in the heart. Changes in these transcripts might occur in response to tissue insult or dysfunction, and may under acute conditions play a role in tissue remodeling (Krajnak et al. 2011; Roberts et al. 2014). These cardiac gene expression alterations may be attributed to (1) direct effects of graphene exposure systemically, (2) the result of changes in blood pressure because of reduced sensitivity to constricting factors, or (3) changes in the electrolyte or fluid balances due to in kidney function alterations. Exposure to GO and rGO also induced changes in pro-inflammatory gene expression in the kidney. Reduced GO-exposed mice also displayed an elevation in the dopamine 1-receptor (*Drd1*) and reduction in the dopamine 2-receptor (*Drd2*). Decreases in expression of *Drd2* receptors have been linked to a kidney injury (Zhang et al. 2016b), and a change in the ratio between Drd1 and Drd2 receptors, leading to modifications in blood volume and circulating sodium levels (Banday and Lokhandwala 2009; Chugh, Lokhandwala, and Asghar 2012; Gildea et al. 2014; Yang et al. 2014), which subsequently affect cardiac function (Banday and Lokhandwala 2009; Chugh, Lokhandwala, and Asghar 2012; Yang et al. 2014).

Evidence indicates that pulmonary exposure to graphene nanoparticles might exert an acute effect on peripheral and cardiovascular systems (Donaldson et al. 2013), particularly the oxidized forms of the material. Depending upon the form and size of the particle, pulmonary exposure to graphene or other particles may affect vascular function by acting on the heart, peripheral blood vessels and renal system (Donaldson et al. 2013; Kan et al. 2014; Kermanizadeh et al. 2016; Knuckles et al. 2012; LeBlanc et al. 2010; McKinney et al. 2012; Nurkiewicz et al. 2006; Roberts et al. 2013; Saber et al. 2013). The effects noted are a result of an acute exposure to a high dose of graphene and suggest that prolonged exposures might contribute to the development of cardiac and/or renal failure. The physiological and cellular responses initiated by graphene appear to be dependent on size and oxidation state of the materials [this experiment and (Roberts et al. 2016)]. Further particle load in the lung may also be a significant factor. On a mass-based dose model, as the size of the particle is reduced, there is an increase in the number of particles delivered to the lungs and consequently an elevated pulmonary particle load (Anderson et al. 2015; Ma-Hock et al. 2013). Based upon these physical properties of the particle, it is not surprising that in Experiment 1, the most pronounced effect was with CB, which was the smallest primary particle and the particle had the highest particle number load. In Experiment 2, the effects of graphene were more pronounced in the rGO-exposed mice. Although the agglomerate size of the oxidized materials did not differ markedly when dispersed in DM, the high surface area and low density of the rGO material relative to the GO might result a greater particle load by number when delivered at a similar mass, as performed in these studies; therefore, the influence of particle load may also be a factor in the responses observed in this treatment group (Han et al. 2015; Kim et al. 2016; Long, Nascarella, and Valberg 2013; Schinwald et al. 2012; Shin et al. 2015; Tabor et al. 2016).

Data suggest that pulmonary exposure to graphene at the dose used in this study exerted acute effects on the cardiovascular and renal systems. If the changes induced by this acute exposure persist with repeated exposures, it is possible that the physiological and cellular responses observed might lead to injury or dysfunction of the cardiovascular and renal systems. Roberts et al. (2016) showed that the dose of Gr20 used in this study produced an increase in markers of pulmonary inflammation (Roberts et al. 2016). There are few studies on oxidized forms of graphene, but based upon the results these and published data (Han et al. 2015), it is likely that exposure to a high dose

may result in the potential for pro-longed pulmonary inflammation affecting the cardiovascular and renal systems; However, longer term studies with additional doses and time points need to be performed. It is also important to note that there are currently few studies that examine workplace exposure levels in graphene manufacturing and handling, where the risk of exposure is likely higher than that encountered by release in the environment. Therefore, more exposure assessment studies are necessary to fully assess the risk associated with a potential workplace and environmental exposure along the life cycle of graphene nanomaterials (Dasari Shareena et al. 2018; Ghio, Carraway, and Madden 2012).

## Disclaimer

The findings and conclusions in this report are those of the authors and do not necessarily represent the official position of the National Institute for Occupational Safety and Health, Centers for Disease Control and Prevention.

## References


Anderson, D. S., E. S. Patchin, R. M. Silva, D. L. Uyeminami, A. Sharmah, T. Guo, G. K. Das, J. M. Brown, J. Shannahan, T. Gordon, et al. 2015. Influence of particle size on persistence and clearance of aerosolizeed silver naoparticles in the rat lung. *Toxicol. Sci.* 144:366–81. doi:10.1093/toxsci/kfv005.

Banday, A. A., and M. F. Lokhandwala. 2009. Inhibition of natriuretic factors increases blood pressure in rats. *Am. J. Physiol. Renal Physiol.* 297:F397–F402. doi:10.1152/ajprenal.90729.2008.

Bengtson, S., K. B. Knudsen, Z. O. Kyjovsla, T. Berthing, V. Slaug, M. Levin, I. K. Koponen, A. Shivayogimath, T. J. Booth, B. Alonso, et al. 2017. Differences in inflammation and acute phase response but similar genotoxicity in mice following pulmonary exposure to graphe oxide and reduced graphine oxide. *PLoS ONE.* 12:e0178355. doi:10.1371/journal.pone.0178355.

Bussy, C., D. Jasim, N. Lozano, D. Terry, and K. Kostarelos. 2015. The current graphene safety landscape-a literature mining exercise. *Nanoscale.* 7:2015. doi:10.1039/C5NR00236B.

Chugh, G., M. F. Lokhandwala, and M. Asghar. 2012. Altered functioning of both renal dopamine D1 and angiotensin II type 1 receptors causes hypertension in old rats. *Hypertension.* 59:1029–36. doi:10.1161/HYPERTENSIONAHA.112.192302.

Croft, D. P., S. J. Cameron, C. N. Morrell, C. J. Lowenstein, F. Ling, W. Zareba, P. K. Hopke, M. J. Utell, S. W. Thurston, K. Thevenet-Morrison, et al. 2017. Associations between ambient wood smoke and other particulate pollutants and biomarkers of systemic inflammation, coagulation and thrombosis in cardiac patients. *Environ. Res.* 154:352–61. doi:10.1016/j.envres.2017.01.027.

Dasari Shareena, T. P., D. McShan, A. K. Dasmahapatra, and P. B. Tchounwou. 2018. A review on graphene-based nanomaterials in biomedical applications and risks in environment and health. *Nanomicro. Lett.* 10. doi:10.1007/s40820-018-0206-4.

Demir, E., and R. Marcos. 2018. Toxic and genotoxic effects of graphene and multi-walled carbon nanotubes. *J. Toxicol. Environ. Health, Part A.* 81:645–60. doi:10.1080/15287394.2018.1477314.

Donaldson, K., R. Duffin, J. P. Langrish, M. R. Miller, N. L. Mills, C. A. Poland, J. Raftis, A. Shah, C. A. Shaw, and D. E. Newby. 2013. Nanoparticles and the cardiovascular system: A critical review. *Nanomedicine (Lond).* 8:403–23. doi:10.2217/nnm.13.16.

Duch, M. C., G. R. Budinger, Y. T. Liang, S. Soberanes, D. Urich, S. E. Chiarella, L. A. Campochiaro, A. Gonzalez, N. S. Chandel, M. C. Hersam, et al. 2011. Minimizing oxidation and stable nanoscale dispersion improves the biocompatibility of graphene in the lung. *Nano Lett.* 11:5201–07. doi:10.1021/nl202515a.

Erdely, A., M. Dahm, B. T. Chen, P. C. Zeidler-Erdely, J. E. Fernback, M. E. Birch, D. E. Evans, M. L. Kashon, J. A. Deddens, T. Hulderman, et al. 2013. Carbon nanotube dosimetry: From workplace exposure assessment to inhalation toxicology. *Part Fibre Toxicol.* 10:53. doi:10.1186/1743-8977-10-56.

Feng, L., and Z. Liu. 2011. Graphene in biomedicine: Opportunities and challenges. *Nanomedicine (Lond).* 6:317–24. doi:10.2217/nnm.10.158.

Ghio, A. J., M. S. Carraway, and M. C. Madden. 2012. Composition of air pollution particles and oxidative stress in cells, tissues, and living systems. *J. Toxicol. Environ. Health, Part B.* 15:1–21. doi:10.1080/10937404.2012.632359.

Gildea, J. J., I. T. Shah, R. VanSciver, J. A. Israel, C. Enzensperger, H. E. McGrath, P. A. Jose, and R. A. Felder. 2014. The cooperative roles of the dopamine receptors D1R and D5R, on the regulation of renal sodium transport. *Kidney Int.* 86:118–26. doi:10.1038/ki.2014.5.

Han, S. G., J. K. Kim, J. H. Shin, J. H. Hwang, J. S. Lee, T. G. Kim, J. H. Lee, G. H. Lee, K. S. Kim, H. S. Lee, et al. 2015. Pulmonary responses of sprague-dawley rats in single inhalation exposure to graphene oxide nanomaterials. *Biomed. Res. Int.* 2015:376756. doi:10.1155/2015/376756.

Holz, O., K. Heusser, M. Muller, H. Windt, K. Schwarz, C. Schindler, J. Tank, J. M. Hohlfeld, and J. Jordan. 2018. Airway and system inflammatory responses to ultafine carbon black particles and ozone in older health subjects. *J. Toxicol. Environ. Health, Part A.* 18:576–88. doi:10.1080/15287394.2018.1463331.

Kan, H., Z. Wu, Y. C. Lin, T. H. Chen, J. L. Cumpston, M. L. Kashon, S. Leonard, A. E. Munson, and V. Castranova. 2014. The role of nodose ganglia in the regulation of cardiovascular function following pulmonary

exposure to ultrafine titanium dioxide. *Nanotoxicology*. 8:447–54. doi:10.3109/17435390.2013.796536.

Kermanizadeh, A., I. Gosens, L. MacCalman, H. Johnston, P. H. Danielsen, N. R. Jacobsen, A. G. Lenz, T. Fernandes, R. P. Schins, F. R. Cassee, et al. 2016. A multilaboratory toxicological assessment of a panel of 10 engineered nanomaterials to human health–ENPRA Project–The highlights, limitations, and current and future challenges. *J. Toxicol. Environ. Health, Part B*. 19:1–28. doi:10.1080/10937404.2015.1126210.

Kim, J. K., J. H. Shin, J. S. Lee, J. H. Hwang, J. H. Lee, J. E. Baek, T. G. Kim, B. W. Kim, J. S. Kim, G. H. Lee, et al. 2016. 28-Day inhalation toxicity of graphene nanoplatelets in Sprague-Dawley rats. *Nanotoxicology*. 10:891–901. doi:10.3109/17435390.2015.1133865.

Knuckles, T. L., J. Yi, D. G. Frazer, H. D. Leonard, B. T. Chen, V. Castranova, and T. R. Nurkiewicz. 2012. Nanoparticle inhalation alters systemic arteriolar vasoreactivity through sympathetic and cyclooxygenase-mediated pathways. *Nanotoxicology*. 6:724–35. doi:10.3109/17435390.2011.606926.

Kotsonis, P., A. Frey, L. G. Frolich, H. Hofman, A. Reif, D. A. Wink, M. Feelisch, and H. H. Schmidt. 1999. Autoinhibition of neuronal nitric oxide synthase: Distinct effects of reactive nitrogen and oxygen species on enzyme activity. *Biochem. J.* 340:745–52.

Krajnak, K., H. Kan, S. Waugh, G. R. Miller, C. Johnson, J. R. Roberts, W. T. Goldsmith, M. Jackson, W. McKinney, D. Frazer, et al. 2011. Acute effects of COREXIT EC9500A on cardiovascular functions in rats. *J. Toxicol. Environ. Health Part A*. 74:1397–404. doi:10.1080/15287394.2011.606795.

LeBlanc, A. J., A. M. Moseley, B. T. Chen, D. Frazer, V. Castranova, and T. R. Nurkiewicz. 2010. Nanoparticle inhalation impairs coronary microvascular reactivity via a local reactive oxygen species-dependent mechanism. *Cardiovasc. Toxicol.* 10:27–36. doi:10.1007/s12012-009-9060-4.

Lee, J. H., J. H. Han, J. H. Kim, B. Kim, D. Bello, J. K. Kim, G. H. Lee, E. K. Sohn, K. Lee, K. Ahn, et al. 2016. Exposure monitoring of graphene nanoplatelets manufacturing workplaces. *Inhal. Toxicol.* 28:281–91. doi:10.3109/08958378.2016.1163442.

Li, B., J. Yang, Q. Huang, Y. Zhang, C. Peng, Y. Zhang, Y. He, J. Shi, W. Li, J. Hu, et al. 2013. Biodistribution and pulmonary toxicity of intratracheally instilled graphene oxide in mice. *NPG Asia Materials*. 5:e44. doi:10.1038/am.2013.7.

Li, R., L. M. Guiney, C. H. Chang, N. D. Mansukhani, Z. Ji, X. L. Wang, Y.-P. Liao, W. Jiang, B. Sun, M. C. Hersam, et al. 2018. Surface oxidation and graphene oxide determines membrane damage, lipid peroxidation and cytotoxicity in macrophages in a pulmonary toxicity model. *ACS Nano*. 12:1390–402. doi:10.1021/acsnano.7b07737.

Liang, M., M. Hu, B. Pan, Y. Xie, and E. J. Petersen. 2016. Biodistribution and toxicity of radio-labeled few layer graphene in mice after intratracheal instillation. *Part Fibre Toxicol.* 13:7–18. doi:10.1186/s12989-016-0120-1.

Long, C. M., M. A. Nascarella, and P. A. Valberg. 2013. Carbon black vs. black carbon and other airborne materials containing elemental carbon: Physical and chemical distinctions. *Environ. Pollut.* 181:271–86. doi:10.1016/j.envpol.2013.06.009.

Lovinsky-Desir, S., K. H. Jung, A. G. Rundle, L. A. Hoepner, J. B. Bautista, F. P. Perera, S. N. Chillrud, M. S. Perzanowski, and R. L. Miller. 2016. Physical activity, black carbon exposure and airway inflammation in an urban adolescent cohort. *Environ. Res.* 151:756–62. doi:10.1016/j.envres.2016.09.005.

Lyu, L., H. Wang, B. Li, Q. Qin, L. Qi, M. Nagarkatti, P. Nagarkatti, J. S. Janicki, X. L. Wang, and T. Cui. 2015. A critical role of cardiac fibroblast-derived exosomes in activating renin angiotensin system in cardiomyocytes. *J. Mol. Cell. Cardiol.* 89:268–79. doi:10.1016/j.yjmcc.2015.10.022.

Ma-Hock, L., V. Strauss, S. Treumann, K. Kuttler, W. Wohlleben, T. Hofmann, S. Groters, K. Wiench, B. van Ravenzwaay, and R. Landsiedel. 2013. Comparative inhalation toxicity of multi-wall carbon nanotubes, graphene, graphite nanoplatelets and low surface carbon black. *Part Fibre Toxicol.* 10:23. doi:10.1186/1743-8977-10-56.

Mao, L., M. Hu, B. Pan, Y. Xie, and E. J. Petersen. 2016. Biodistrubtion and toxicity of ratio-labeled few layer graphene in mice after intratracheal installation. *Part Fibre Toxicol.* 13:1–12. doi:10.1186/s12989-015-0112-6.

Materials AsoT. 2002. Standard test method for metal powder specifc surface area by physical adsorption, vol ASTM B922-02, ASTM InternationalWest Conshohocken, PA.

McKinney, W., M. Jackson, T. M. Sager, J. S. Reynolds, B. T. Chen, A. Afshari, K. Krajnak, S. Waugh, C. Johnson, R. R. Mercer, et al. 2012. Pulmonary and cardiovascular responses of rats to inhalation of a commercial antimicrobial spray containing titanium dioxide nanoparticles. *Inhal. Toxicol.* 24:447–57. doi:10.3109/08958378.2012.685111.

Mukherjee, S., P. Sriram, A. K. Barui, S. K. Nethi, V. Veeriah, S. Chatterjee, K. Ittara, I. Suresh, and C. R. Patra. 2015. Graphene oxides show angiogenic properties. *Adv. Healthcare Mater.* 4:1722–32. doi:10.1002/adhm.201500155.

Nurkiewicz, T. R., D. W. Porter, M. Barger, L. Millecchia, K. M. Rao, P. J. Marvar, A. F. Hubbs, V. Castranova, and M. A. Boegehold. 2006. Systemic microvascular dysfunction and inflammation after pulmonary particulate matter exposure. *Environ. Health Perspect.* 114:412–19. doi:10.1289/ehp.8413.

O'Mahony, C., E. U. Haq, C. Sillien, and S. A. M. Tofail. 2019. Rheological issues in carbon-based inks for additive manufacturing. *Micromachines (Basel)*. 10:99–123. doi:10.3390/mi10020099.

Porter, D. W., A. F. Hubbs, R. R. Mercer, N. Wu, M. G. Wolfarth, K. Sriram, S. Leonard, L. Battelli, D. Schwegler-Berry, S. Friend, et al. 2010. Mouse pulmonary dose- and time course-responses induced by exposure

to multi-walled carbon nanotubes. *Toxicology.* 269:136–47. doi:10.1016/j.tox.2009.10.017.

Roberts, J. R., S. E. Anderson, H. Kan, K. Krajnak, J. A. Thompson, A. Kenyon, W. T. Goldsmith, W. McKinney, D. G. Frazer, M. Jackson, et al. 2014. Evaluation of pulmonary and systemic toxicity of oil dispersant (COREXIT EC9500A((R))) following acute repeated inhalation exposure. *Environ. Health Insights.* 8 (Suppl 1):63–74. doi:10.4137/EHI.S15262.

Roberts, J. R., W. McKinney, H. Kan, K. Krajnak, D. G. Frazer, T. A. Thomas, S. Waugh, A. Kenyon, R. I. MacCuspie, V. A. Hackley, et al. 2013. Pulmonary and cardiovascular responses of rats to inhalation of silver nanoparticles. *J. Toxicol. Environ. Health Part A.* 76:651–68. doi:10.1080/15287394.2013.792024.

Roberts, J. R., R. R. Mercer, A. B. Stefaniak, M. S. Seehra, U. K. Geddam, I. S. Chaudhuri, A. Kyrlidis, V. K. Kodali, T. Sager, A. Kenyon, et al. 2016. Evaluation of pulmonary and systemic toxicity following lung exposure to graphite nanoplates: A member of the graphene-based nanomaterial family. *Part. Toxicol.* 13:s1289-016–0145-5.

Saber, A. T., J. S. Lamson, N. R. Jacobsen, G. Ravn-Haren, K. S. Hougaard, A. N. Nyendi, P. Wahlberg, A. M. Madsen, P. Jackson, H. Wallin, et al. 2013. Particle-induced pulmonary acute phase response correlates with neurotrophil influx linking inhaled particles and cardiovascular risk. *PLoS ONE.* 8:e69020. doi:10.1371/journal.pone.0069020.

Sager, T. M., D. W. Porter, V. A. Robinson, W. G. Lindsley, D. E. Schwegler-Berry, and V. Castranova. 2007. Improved method to disperse nanoparticles for *in vitro* and *in vivo* investigation of toxicity. *Nanotoxicology.* 1:118–29. doi:10.1080/17435390701381596.

Sanchez, V. C., A. Jachak, R. H. Hurt, and A. B. Kane. 2012. Biological interactions of graphene-family nanomaterials-An interdisciplinary review. *Chem. Res. Toxicol.* 13:15–34. doi:10.1021/tx200339h.

Sang Tran, T., N. K. Dutta, and N. Roy Choudhury. 2019. Graphene-based inks for printing of planar micro-supercapacitors: A review. *Materials (Basel).* 12:978–99. doi:10.3390/ma12060978.

Schinwald, A., F. A. Murphy, A. Jones, W. MacNee, and K. Donaldson. 2012. Graphene-based nanoplatelets: A new risk to the respiratory system as a consequence of their unusual aerodynamic properties. *ACS Nano.* 6:736–46. doi:10.1021/nn204229f.

Shin, J. H., S. G. Han, J. K. Kim, B. W. Kim, J. H. Hwang, J. S. Lee, J. H. Lee, J. E. Baek, T. G. Kim, K. S. Kim, et al. 2015. 5-Day repeated inhalation and 28-day post-exposure study of graphene. *Nanotoxicology.* 9:1023–31. doi:10.3109/17435390.2014.998306.

Shurin, M. R., N. Yanamala, E. R. Kisin, A. V. Tkach, G. V. Shurin, A. R. Murray, H. D. Lenard, J. S. Reynolds, D. W. Gutin, and A. Star. 2014. Graphene oxide attenuates Th2-type immune responses, but augments airway remodeling and hyperresponsiveness in a murine model of asthma. *ACS Nano.* 8:2014. doi:10.1021/nn406454u.

Smith, S. 2017. The global market for graphene. Future markets: PRNewswire. https://www.marketwatch.com/press-release/the-global-market-for-graphene-2017-10-26

Su, W.-C., B.-K. Ku, P. Kulkarni, and Y. S. Cheng. 2016. Deposition of graphene nanoparticles in human upper airways. *J. Occup. Environ. Med.* 13:48–59.

Tabish, T. A., S. Zhang, and P. G. Winyard. 2018. Developing the next generation of graphene-based plaforms for cancer therapuetics: The potential role of reactive oxygen species. *Redox Biol.* 15:34–40.

Tabor, C. M., C. A. Shaw, S. Robertson, M. R. Miller, R. Duffin, K. Donaldson, D. E. Newby, and P. W. Hadoke. 2016. Platelet activation independent of pulmonary inflammation contributes to diesel exhaust particulate-induced promotion of arterial thrombosis. *Part Fibre Toxicol.* 13:6.

Xia, Y., V. L. Dawson, T. M. Dawson, S. H. Snyder, and I. L. Zweier. 1996. Nitric oxide synthase generates superoxide and nitric oxide in arginine-depleted cells leading to peroxynitrite-mediated cellular injury. *Proc. Natl. Acad. Sci. USA.* 93:677–6774.

Yang, Y., S. Cuevas, S. Yang, V. A. Villar, C. Escano, L. Asico, P. Yu, X. Jiang, E. J. Weinman, I. Armando, et al. 2014. Sestrin2 decreases renal oxidative stress, lowers blood pressure, and mediates dopamine D2 receptor-induced inhibition of reactive oxygen species production. *Hypertension.* 64:825–32.

Zhang, B., P. Wei, Z. Zhou, and T. Wei. 2016a. Interactions of graphene with mammalian cells: Molecular mechanisms and biomedical insights. *Adv Drug Del Rev.* 105:145–62.

Zhang, Y., X. Jiang, C. Qin, S. Cuevas, P. A. Jose, and I. Armando. 2016b. Dopamine D2 receptors' effects on renal inflammation are mediated by regulation of PP2A function. *Am. J. Physiol. Renal Physiol.* 310:F128–F134.